A simple chemical route toward monodisperse iron carbide nanoparticles displaying tunable magnetic and unprecedented hyperthermia properties

Anca Meffre, Boubker Mehdaoui, Vinciane Kelsen, Pier Francesco Fazzini, Julian Carrey, Sebastien Lachaize, Marc Respaud*, Bruno Chaudret*

Laboratoire de Physique et Chimie des Nano Objets, INSA, Université de Toulouse, 135, avenue de Rangueil, F-31077 Toulouse, France

SUPPORTING INFORMATION

METHODS

All synthesis of non-commercial compounds were performed under argon by using Fischer-Porter bottles techniques, a glove box and argon/vacuum lines. Mesitylene (99%), toluene (99%), tetrahydrofurane (99%) and pentane (99%) were purchased from VWR Prolabo, then purified on alumina desiccant and degassed through three freeze-pump-thaw cycles. The commercial products, hexadecylammine (HDA, 99%), hydrochloric acid in diethylether (HCl, 1mol l^{-1}) were purchased from Sigma-Aldrich, $Fe(CO)_5$ (99,5%) from Acros organics. The bis(amido)iron(**II**) dimer $\{Fe[N(SiMe_3)_2]_2\}_2$ was purchased from Nanomeps. All these compounds were used without any additional purification.

CHARACTERIZATION

We characterized the size, the morphology and the structure of as-synthesized samples by transmission electronic microscopy TEM and high-resolution transmission electronic microscopy (HRTEM). Conventional bright-field images were performed using JEOL microscopes (Model 1400F) working at 100kV and HRTEM was conducted on a FEI Tecnai-F20 microscope working at 200kV. XRD measurements were performed on a PANalytical Empyrean diffractometer using Co-Kα radiation at 45kV and 40mA.

The magnetization of the samples was measured on a Quantum Design Model MPMS 5.5 SQUID magnetometer. The absolute magnetization was deduced from the iron(0) content determined by microanalysis using inductively coupled plasma mass spectrometry technique (ICP). The iron state and its environment were analyzed by Mossbauer spectroscopy (WISSEL, ^{57}Co source). These studies were carried out on powder samples that were prepared and sealed under an argon atmosphere.

CHEMICAL SYNTHESIS

HDAHCl preparation

The hexadecylammonium chloride (HADHCl) was prepared according to a published procedure. Addition of the HCl in diethylether (15 ml, 1.5 mmol of HCl) to a pentane solution (50 mL) of HDA (2.4 mg, 1 mmol) led to the immediate precipitation of a white solid that was filtered off, washed three times with THF (15 mL) and dried under vacuum overnight. The yield was 82% (2.3 mg).

Typical procedures leading to MM1(iron carbide nanoparticles)

In a typical synthesis, the synthesis of preformed iron NPs was made as follows: in the glove box, 1.5 mmol of HDAHCl (415.5 mg) and mmol of HDA (483 mg) were added to a green solution of 0.5 mmol $\{Fe[N(SiMe_3)_2]_2\}_2$ (376.5 mg) in 20 ml of distilled and degassed mesitylene in a Fischer Porter bottle. The bottle is then placed in an oil bath at 150°C for 48h, and thus the reaction mixture under Argon atmosphere was heated under vigorous magnetic stirring. At the end of the reaction, 0.5 mmol of $Fe(CO)_5$ are added on the raw solution. The bottle is conditioned under H_2 at a pressure of 3 bars for **MM1**. The reaction mixture is placed again in an oil bath at 150°C. After 24h under vigorous magnetic stirring a very magnetic black material was found on the stirring bar. The black solution is removed, and the magnetic material (**MM1**) collected was washed 5 times with 15 ml of distilled and degassed toluene, and then dried under vacuum. Considering the weight fraction of iron metal of the sample 86% for **MM1** the yield related can be calculated as 82%.

Typical procedures leading to MM2 (core/shell iron/iron carbide nanoparticles)

Core-shell Fe/Fe_xC_y nano-objects was formed by carrying out the decomposition of $Fe(CO)_5$ under Ar at 150°C. In a typical synthesis 0.5 mmol of $Fe(CO)_5$ are added on the raw solution of preformed iron nanoparticles about 9.6 nm. The bottle is conditioned under Ar **(pressure?).** The reaction mixture was placed again in an oil bath at 150°C. After 24h under vigorous magnetic stirring a very magnetic black material was found on the stirring bar. The black solution was removed, and the magnetic material (**MM2**) collected was washed 5 times with 15 ml of distilled and degased toluene, and then dried under vacuum. TEM and HRTEM analysis (see Fig. 1a,c-article) combined with Mossbauer spectra (see Fig. 1b-article) and XRD data (see Fig. 1d-article) revealed that starting form iron(0) nanoparticles about 9.6 nm gave in this case core-shell $Fe/(Fe_{2.2}C+ Fe_5C_2)$ nanoparticles about 13.1 nm with a core diameter about 9.3 nm.

A procedure totally similar to that used for **MM1** performed under H_2 but a second step done at low temperature (120°C), led also to magnetic material core/shell iron/iron carbide nanoparticles, **MM2** that contained 80% of iron. Decomposition of 0,5 mmol of $Fe(CO)_5$ on the raw solution of preformed iron(0) nanoparticles about 9.6 nm at 120°C under 3 bars of H_2, gave after 24h to 13.4 nm core/shell iron/iron carbides nanoparticles with a core diameter about 8.4 nm (see Fig S4). The isolated yield was 72%.

HYPERTHERMIA MEASUREMENTS

For a typical hyperthermia experiment, a schlenk containing about 12 mg of powder of iron carbide or iron/iron carbide nanocrystals dispersed in 0.5 ml of mesitylene was filled under inert atmosphere. The schlenk was then placed in a calorimeter with 1.5 ml of deionised water, the temperature of which was measured. The calorimeter was exposed to an alternative magnetic field for a time between 30 and 100s so that the temperature rise never exceeds 20°C. The temperature rise at the end of the magnetic field application was always measured after shaking the calorimeter to ensure the temperature homogeneity, which was measured by putting two probes at the top and the bottom of the calorimeter. The temperature rise was determined after this process from the mean slope of the $\Delta T/\Delta t$ function. Then the SAR values were calculated using the expression:

$$SAR = \frac{\sum_i C_{pi} m_i}{m_{Fe}} \frac{\Delta T}{\Delta t}$$

where C_{pi} and m_i are specific heat capacity and mass for each component respectively (C_p = 449 J $kg^{-1}K^{-1}$ for Fe NPs, C_p = 1750 J $kg^{-1}K^{-1}$ for mesitylene, C_p = 4186 J $kg^{-1}K^{-1}$ for water and C_p = 720 J $kg^{-1}K^{-1}$ for glass), and m_{Fe} is the mass of the pure iron carbide nanocrystals. Dividing *SAR* values by the magnetic field frequency give the specific losses *A*.

The magnetic hyperthermia properties have been also characterized by magnetic hysteresis loops measurement using the setup described in the reference [3]. We used a coil that generates an alternating magnetic field with a variable amplitude and frequency. The essential elements of this setup were pickup coils that recorded induced electromotive forces according to Faraday–Maxwell law of magnetic induction. The amplitude of the alternating magnetic field is obtained using $\mu_0 H_{AC} = \frac{\int e_1 dt}{n S_{coil}}$, where e_1 the voltage at of the empty coil. The magnetization per unit mass σ_S of the nanoparticles is obtained using $\sigma_S = \frac{\int e_2 dt}{\mu_0 n \rho S_{vessel} \Phi}$, where S_{vessel} is the surface of a section of the vessel containing the colloidal solution, Φ the volume concentration of the sample, ρ the magnetic nanoparticles density and e_2 the voltage at the terminal of the two coils in series.

COERCIVE FIELD ANALYSIS

We deduced the effective anisotropy K_{eff} of the nanoparticle from the experimental data using analytical equations for $\mu_0 H_C$ and for $\mu_0 H_{CHyp}$ [1, 2]. For the samples with randomly oriented anisotropy axis, Fe(0) and MM1-1, formula describing nanoparticle with randomly oriented axis (axis aligned with the magnetic field) have been used and the effective anisotropy was deduced from $\mu_0 H_C$ and $\mu_0 H_{CHyp}$ values using $\mu_0 H_C = 0.48 \mu_0 H_K \left(1 - \kappa^{0.8}\right)$, with $\kappa = \frac{k_B T}{KV} \ln\left(\frac{k_B T}{4\mu_0 H_{max} M_S V f \tau_0}\right)$ and $\mu_0 H_K = 2K_{eff} / M_S$.

$$\mu_0 H_{CHyp} = 0.463 \mu_0 H_K \left(1 - \kappa^{0.8}\right),$$

For the samples in which the anisotropy axis are aligned with magnetic field (MM2-1, MM2-2, MM2-3, MM2-4 and MM2-5) the formula $\mu_0 H_C = \mu_0 H_K \left(1 - \kappa^{\frac{1}{2}}\right)$ has been used. For all the samples we assumed a fixed value for $\tau_0 = 10^{-10}$s.

In Table 1 summarizes the main parameters of the samples, as well as the values of the coercive field deduced from magnetic measurements $\mu_0 H_C$, and the coercive field corresponding to the highest slope of the SAR($\mu_0 H_{max}$) curve $\mu_0 H_{CHyp}$.

Note that since only minor loops are measured for Fe(0), MM1-1 and MM2-1 in the available magnetic fields. As a consequence, only an underestimated value of the effective anisotropy can be deduced from the hysteresis loops.

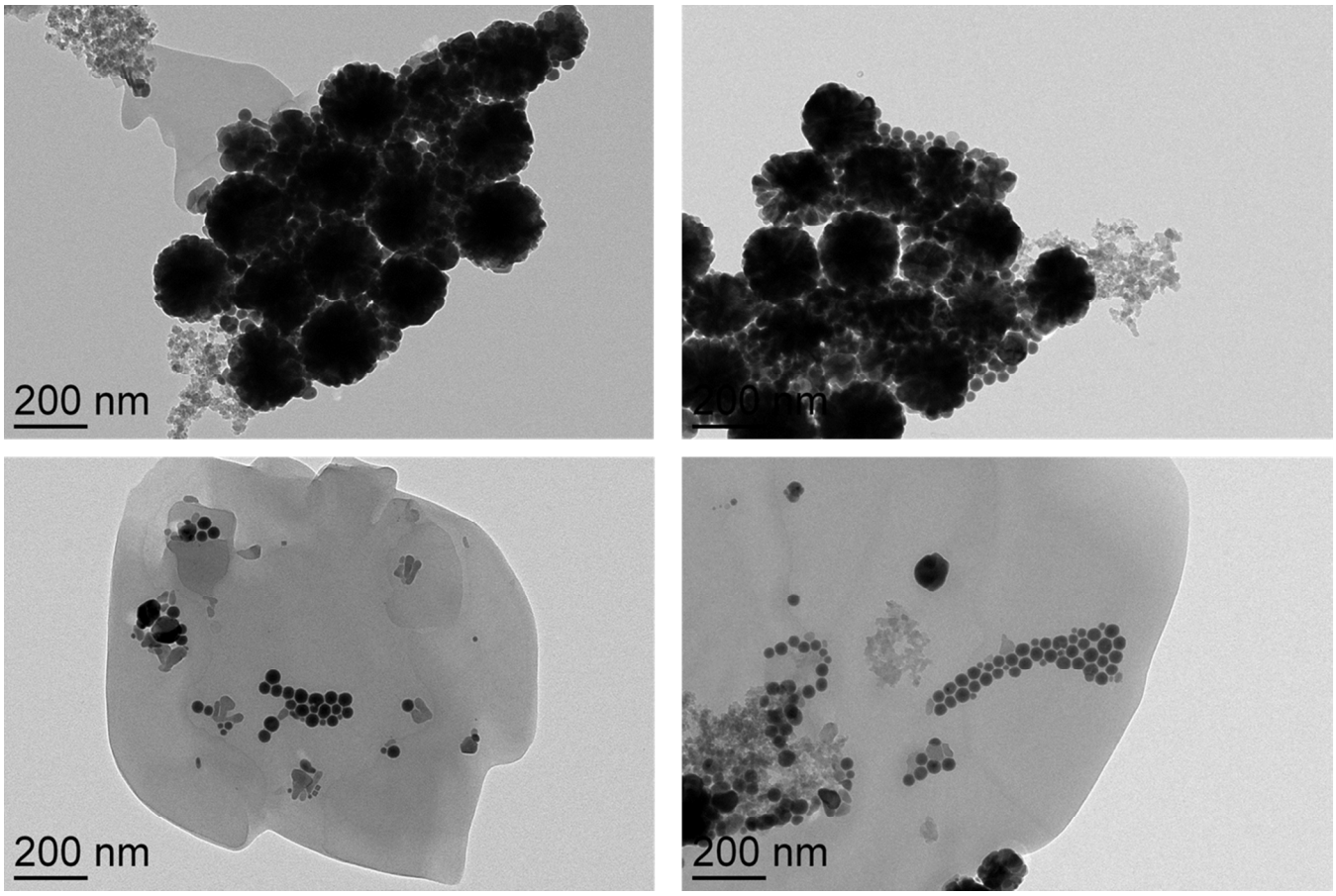

Figure S1. TEM analysis of the material obtained after decomposition of $Fe(CO)_5$/HDAHCl/HDA at 150°C under H2.

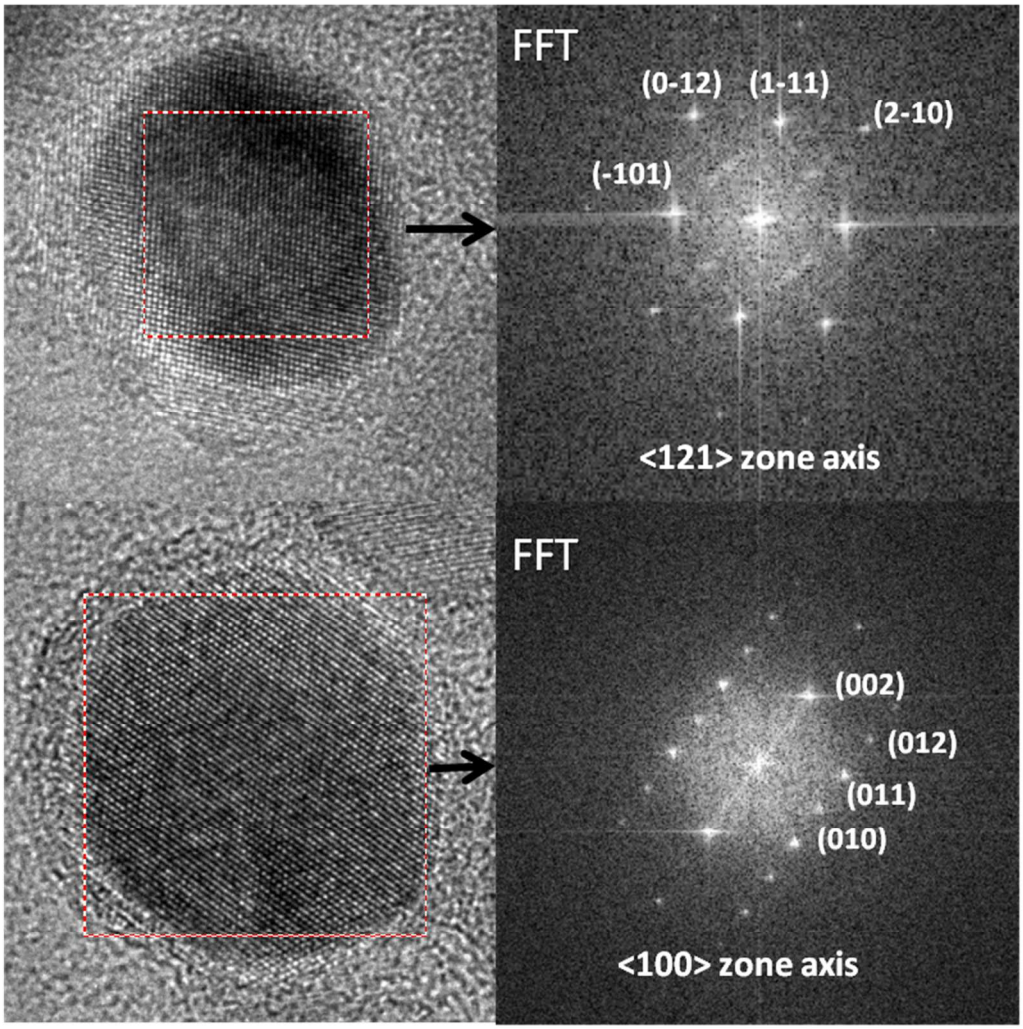

Figure S2. HRTEM analysis of the MM1 material.

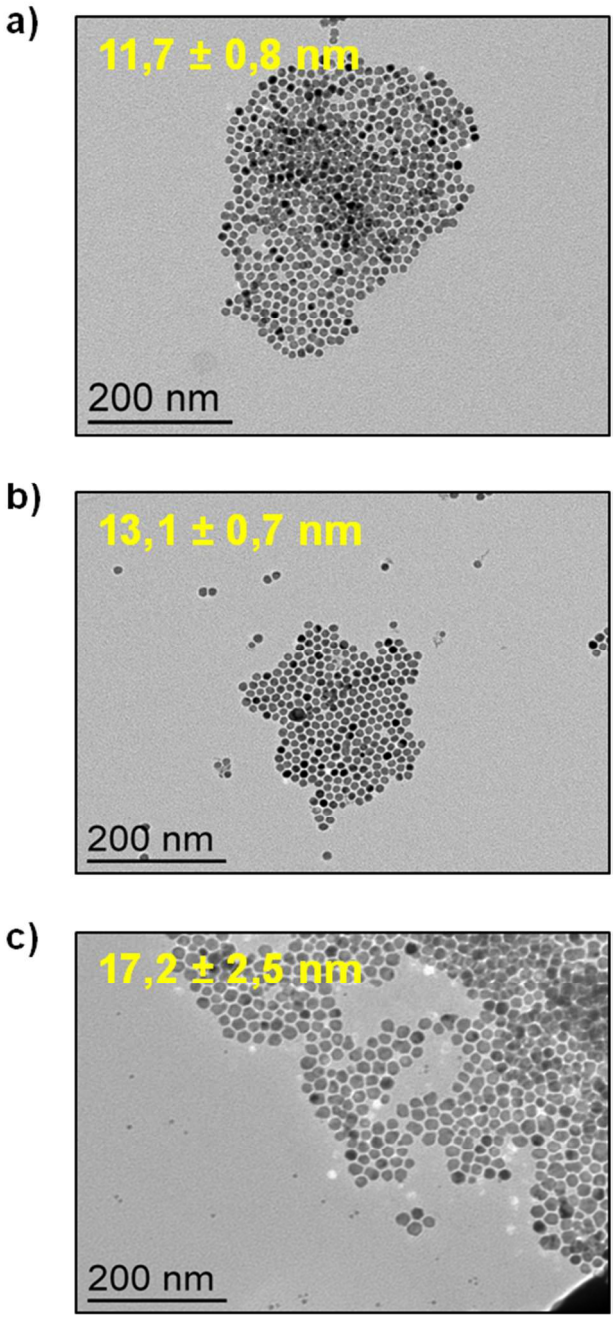

Figure S3. **Tunable size of iron carbide nanocrystals (MM1) by adjusting the size of preformed iron(0) NPs:** (**a**) TEM of ~ 11.7 nm iron carbide nanocrystals obtained by decomposition of 0.5 equivalents of Fe(CO)5 on preformed iron(0) NPs of ~ 8.4 nm at 150°C under H2. (**b**) TEM of ~ 13.1 nm iron carbide nanocrystals obtained by decomposition of 0.5 equivalents of Fe(CO)5 on preformed iron(0) NPs of ~ 9.7 nm at 150°C under H2. (**c**) TEM of ~ 17.2 nm iron carbide nanocrystals obtained by decomposition of 0.5 equivalents of Fe(CO)5 on preformed iron(0) NPs of ~ 11.5 nm at 150°C under H2.

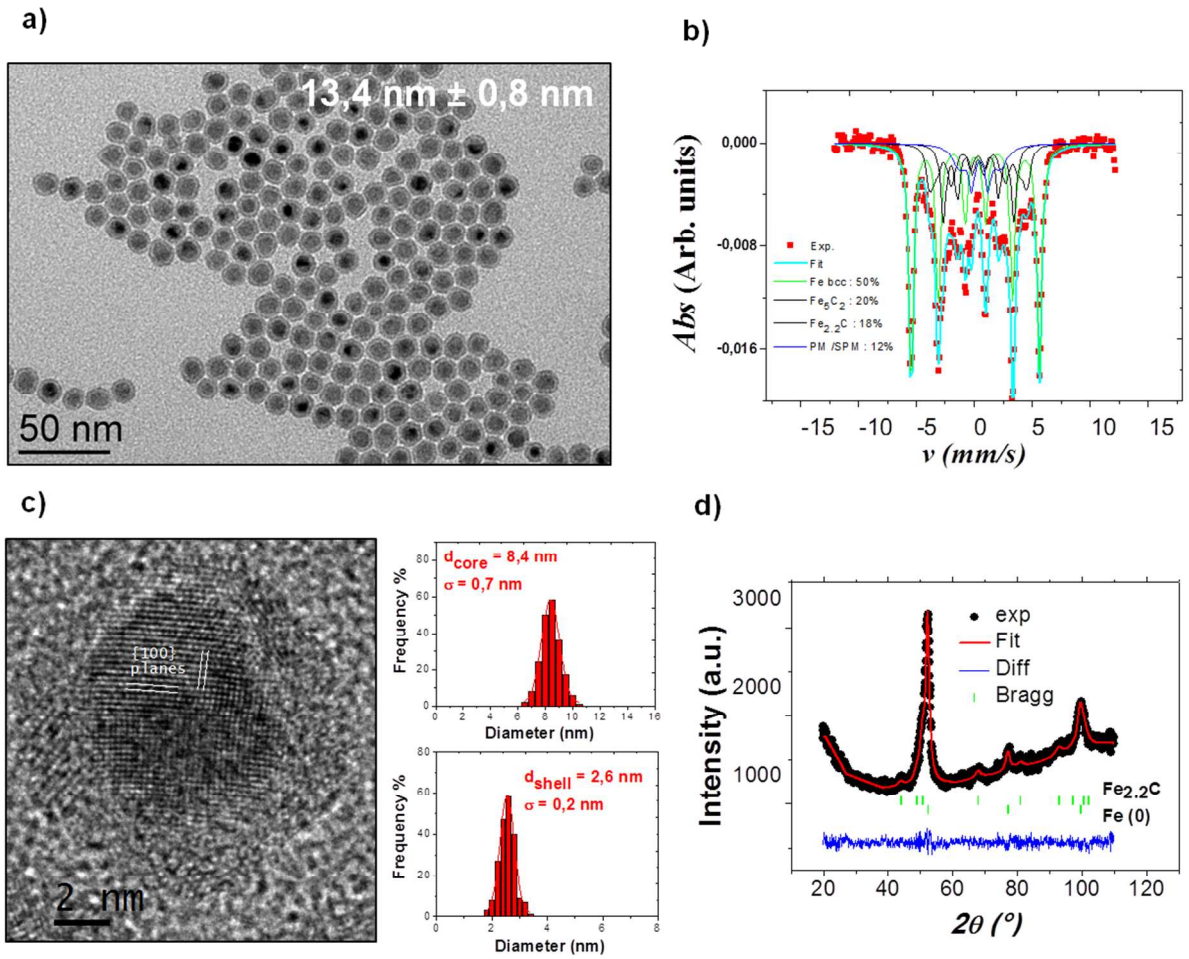

Figure S4. Structural analysis of iron/iron carbide nanoparticles (MM2) of about 13.4 nm: (a) TEM analysis. (**b)** Mossbauer spectrum. (**c)** HRTEM analysis and distribution of the iron(0) core and iron carbide shell. (**d)** Powder-XRD data.

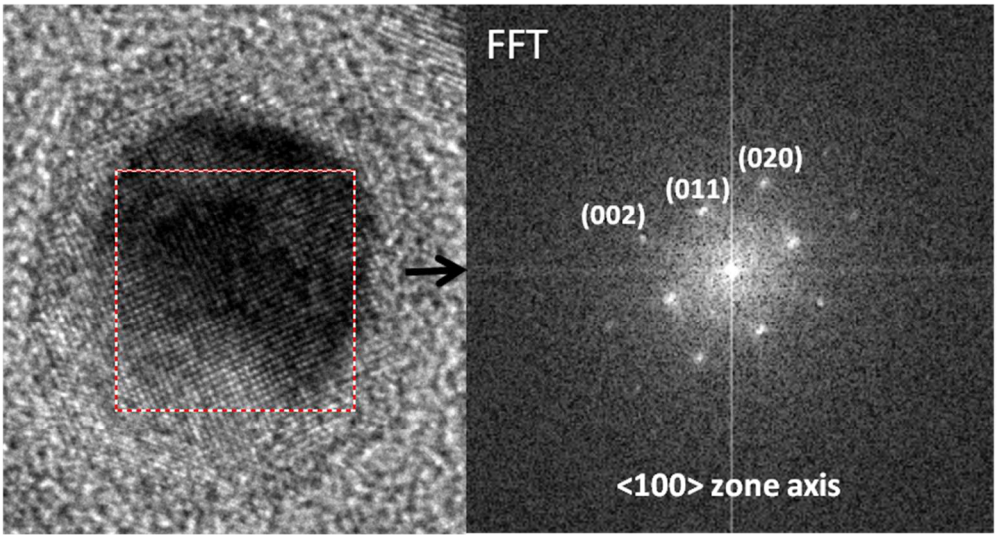

Figure S5. HRTEM analysis of the MM2 material.

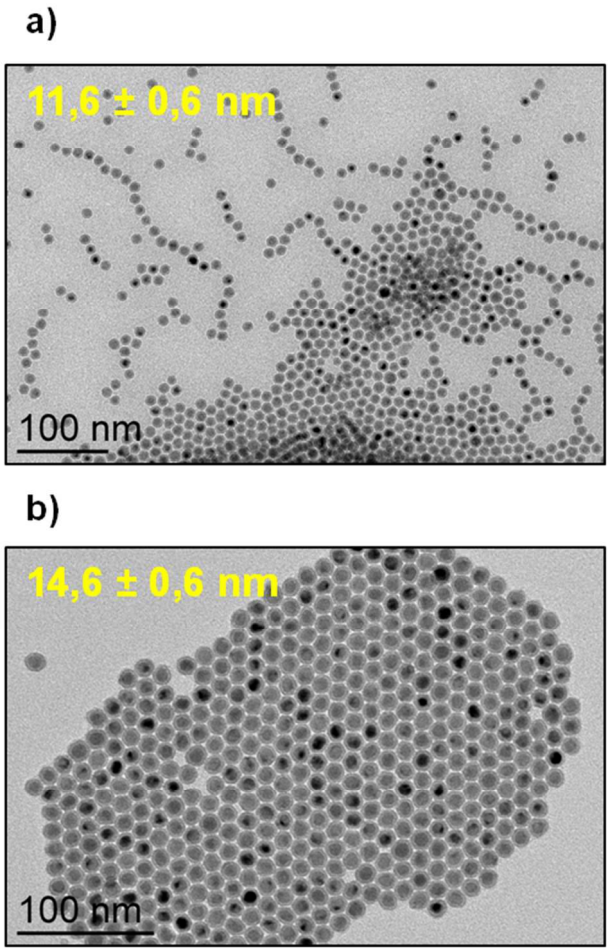

Figure S6. Tunable size of iron/iron carbide nanocrystals (MM2) by adjusting the size of preformed iron(0) NPs: (**a**) TEM of ~ 11.6 nm iron/iron carbide nanocrystals obtained by decomposition of 0.5 equivalents of $Fe(CO)_5$ on preformed iron(0) NPs of ~ 8.5 nm at 150°C under Ar**.(b)** TEM of ~ 14.6 nm iron/iron carbide nanocrystals obtained by decomposition of 2 equivalents of $Fe(CO)_5$ on preformed iron(0) NPs of ~ 9.5 nm at 150°C under Ar.

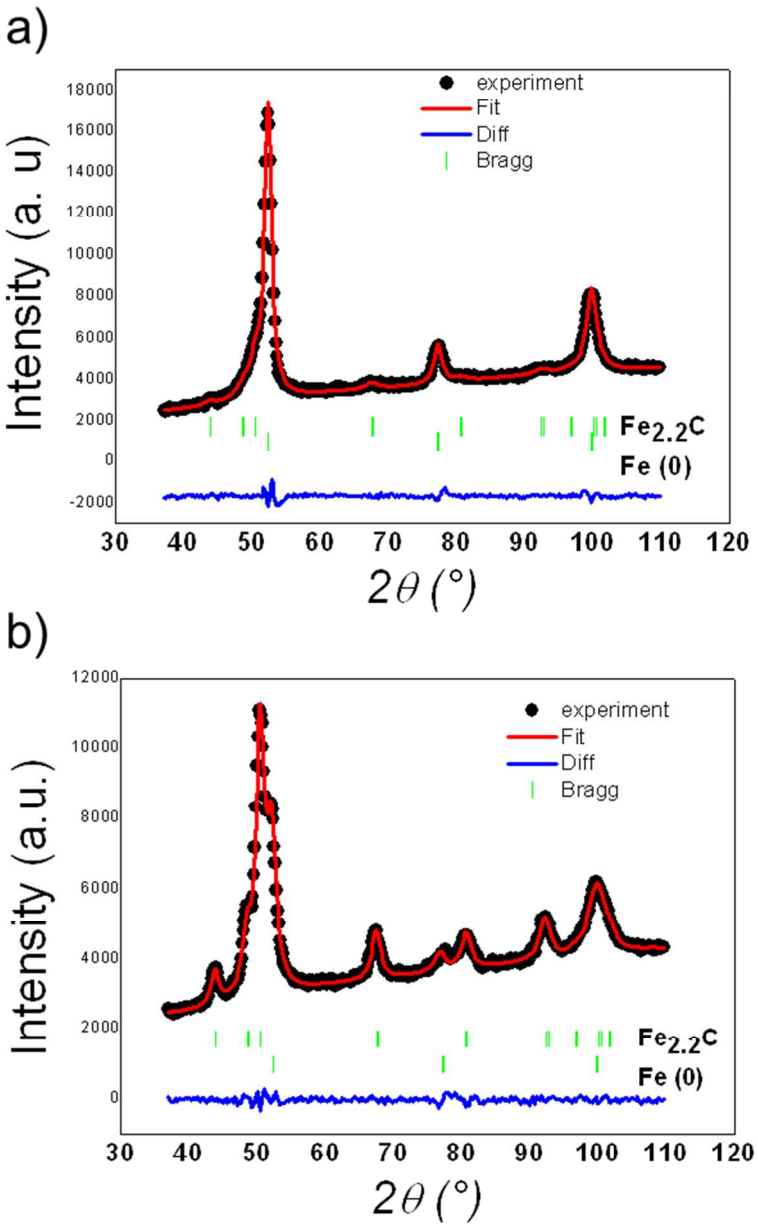

Figure S7. XRD analysis of iron/iron carbide nanoparticles (MM2) obtained at 120°C under H2 after : (a) 24h reaction time. (**b)** 48h reaction time.

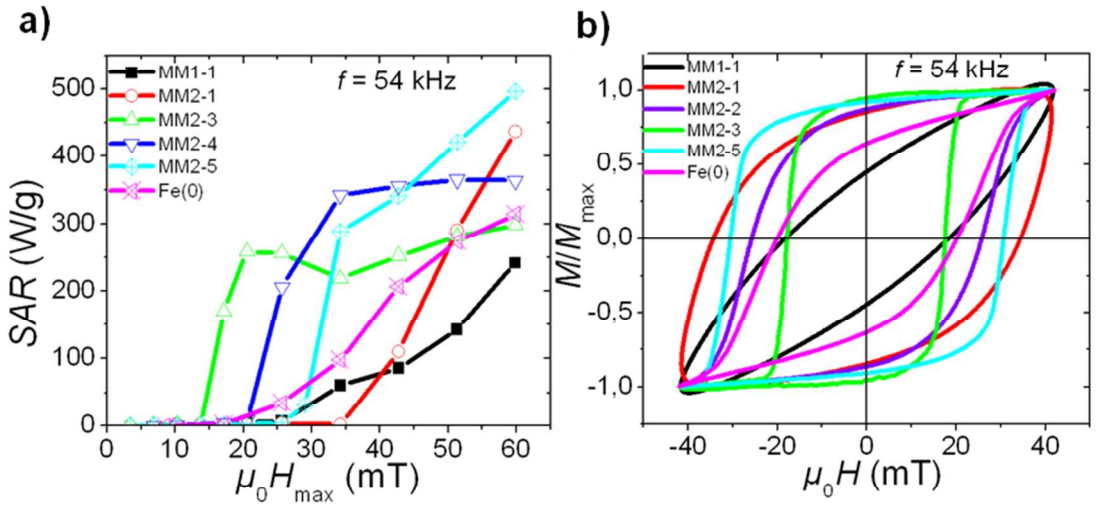

Figure S8. Hyperthermia properties of iron carbide and iron/iron carbide nanocrystals: (a) *SAR* measurements as a function of amplitude of magnetic field at f_{exc} = 54kHz. (b) Normalised hysteresis loops measured at f_{exc} = 54kHz and room temperature for different samples (see Table 1)

Samples	d_0 (nm) TEM	d_{core} (nm) TEM	d_{core} (nm) RX	%$Fe_{2.2}C$ RX	Ms (Am^2/kg)	$\mu_0 H_{cHyp}$ (mT)	$\mu_0 H_{cc}$ ycles (mT)	K_{eff} (J/m^3) hyperthermia	K_{eff} (J/m^3) cycles	*SAR* (20mT) (W/g)	*A* (20mT) (mJ/g)	*α* (20mT)
MM1-1	12.1	*12.1*	*9*	100	146	> 60	> 42	> 117000 3D	> 95200 3D	5.8	*0.1*	0.009
MM2-1	13.5	*10.4*	*7.6*	44	156	50	34	74000 1D	> 60800 1D	1.7	0.31	0.002
MM2-2	13.4	*8.4*	*8.3*	29	-	23	25	56700 1D	58700 1D	51.0	0.94	0.062
MM2-3	13.1	*8.6*	*8.5*	22	202	17	18	54300 1D	55300 1D	258.7	4.79	0.296
MM2-4	12.4	*8.5*	*9.4*	18	198	25	-	68600 1D	-	8.5	0.15	0.009
MM2-5	13.1	*10.6*	*9.4*	16	191	32	30	68200 1D	66220 1D	3.0	0.05	0.003
Fe(0)	13.7	*13.7*	-	0	232	38	20	103700 3D	69000 3D	15.6	0.28	0.015

Table 1. Summary of main morphological properties, magnetic and hyperthermia parameters for different samples: mean diameter d_0 determined by TEM observation, core diameter d_{core} determined by TEM observation and from the X-Ray diffraction (XRD) using the Scherrer equation, $Fe_{2.2}C$ phase fraction deduced from XRD, saturation magnetization *Ms*, coercive field $\mu_0 H_{CHyp}$ deduced from the highest slope of the $SAR(\mu_0 H_{max})$, coercive field $\mu_0 H_C$ deduced from hysteresis loops, effective anisotropy K_{eff} deduced from $\mu_0 H_{CHyp}$ and $\mu_0 H_c$ values using the analytical equations discussed below (1D : analysis considering NPs easy axis aligned with the magnetic field ; 3D: analysis considering NPs easy axis randomly oriented). Specific absorption rate (*SAR*), and losses per cycle *A* measured at f = 54 kHz and $\mu_0 H_{max}$ = 20 mT. Calculated α values using $\alpha = SAR / (4\mu_0 H_{max} M_s f)$.

References:

(1) Mehdaoui, B., Meffre, A., Carrey, J., Lachaize, S., Lacroix, L.-M., Gougeon, M., Chaudret, B., Respaud, M. Optimal Size of Nanoparticles for Magnetic Hyperthermia: A Combined Theoretical and Experimental Study. *Adv. Funct. Mater.* **2011**, *21*, 4573-4581.

(2) Carrey, J., Mehdaoui, B., Respaud, M. Simple models for dynamic hysteresis loop calculations of magnetic single-domain nanoparticles: Application to magnetic hyperthermia optimization, *J. Appl. Phys.* **2011**, *109*, 083921.

(3) Mehdaoui, B; Carrey, J.; Stadler, M; Cornejo, A; Nayral, C; Delpech, F; Chaudret, B; Respaud, M; Influence of a transverse static magnetic field on the magnetic hyperthermia properties and high-frequency hysteresis loops of ferromagnetic FeCo nanoparticles, *Appl. Phys. Lett.* **2012**, 100, 052403